

# Tumor Suppressor INK4: Comparisons of Conformational Properties Between p16<sup>INK4A</sup> and p18<sup>INK4C</sup>

Chunhua Yuan<sup>1</sup>, Junan Li<sup>2</sup>, Thomas L. Selby<sup>1</sup>, In-Ja L. Byeon<sup>3\*</sup> and Ming-Daw Tsai<sup>1,2,3,4\*</sup>

<sup>1</sup>Department of Chemistry  
The Ohio State University  
Columbus, OH 43210, USA

<sup>2</sup>Department of Biochemistry  
The Ohio State University  
Columbus, OH 43210, USA

<sup>3</sup>Campus Chemical Instrument  
Center, The Ohio State  
University, Columbus, OH  
43210, USA

<sup>4</sup>Ohio State Biochemistry  
Program, The Ohio State  
University, Columbus, OH  
43210, USA

The INK4 (inhibitor of cyclin-dependent kinase 4) family consists of four tumor-suppressor proteins: p15<sup>INK4B</sup>, p16<sup>INK4A</sup>, p18<sup>INK4C</sup>, and p19<sup>INK4D</sup>. While their sequences and structures are highly homologous, they show appreciable differences in conformational flexibility, stability, and aggregation tendency. Here, p16 and p18 were first compared directly by NMR for line broadening and disappearance, then investigated by three different approaches in search of the causes of these differences. From denaturation experiments it was found that both proteins are marginally stable with low denaturation stability (1.94 and 2.98 kcal/mol, respectively). Heteronuclear <sup>1</sup>H-<sup>15</sup>N nuclear Overhauser enhancement measurements revealed very limited conformational flexibility on the pico- to nanosecond time-scale for both p16 and p18. H/<sup>2</sup>H exchange of amide protons monitored by NMR on three proteins (p16, p18 as well as p15), however, revealed markedly different rates in the order p18 < p16 ≤ p15. A subset of very slowly exchanging residues (about 19 in total) was identified in p18, including 16 residues in the region of the fourth ankyrin repeat, probably as a result of a stabilizing effect by the extra ankyrin repeat. Thus, while INK4 proteins may have similar low thermodynamic stability as well as limited flexibility on the pico- to nanosecond time-scale, they display pronounced differences in the conformational flexibility on the time-scale of minutes to hours. Further analyses suggested that differences in H/<sup>2</sup>H exchange rates reflect differences in the kinetic stability of the INK4 proteins, which in turn is related to differences in the aggregation tendency.

© 1999 Academic Press

**Keywords:** p16<sup>INK4A</sup>; p18<sup>INK4C</sup>; p15<sup>INK4B</sup>; conformational flexibility of INK4 proteins; conformational stability of INK4 proteins

\*Corresponding authors

Abbreviations used: CD, circular dichroism; CDK, cyclin-dependent kinase; GdnHCl, guanidine hydrochloride; GST, glutathione S-transferase; HSQC, heteronuclear single-quantum coherence; H-T-H, helix-turn-helix; INK4, inhibitor of CDK4; NMR, nuclear magnetic resonance; NOE, nuclear Overhauser effect; NOESY, nuclear Overhauser enhancement correlated spectroscopy; p15, cyclin-dependent kinase inhibitor p15<sup>INK4B</sup>; p16, cyclin-dependent kinase inhibitor p16<sup>INK4A</sup>; p18, cyclin-dependent kinase inhibitor p18<sup>INK4C</sup>; p19, cyclin-dependent kinase inhibitor p19<sup>INK4D</sup>; PF, protection factor.

E-mail addresses of the corresponding authors: Tsai.7@osu.edu; Byeon.2@osu.edu

## Introduction

The inhibitor of cyclin-dependent kinase 4 (INK4) proteins, which bind and inhibit cyclin-dependent kinase (CDK), include four members: p15<sup>INK4B</sup>, p16<sup>INK4A</sup>, p18<sup>INK4C</sup>, and p19<sup>INK4D</sup> (abbreviated as p15, p16, p18, and p19, respectively). Though discovered only a few years ago (Serrano *et al.*, 1993), they have received overwhelming attention in structural and functional studies because p16 is one of the most important tumor suppressor proteins known at present (Sherr, 1996). The p15 and p16 proteins share ~80% sequence identity, while p18 and p19 are only 40–45% identical with each other and with p16 (Byeon *et al.*, 1998). The highest primary sequence conservation is found in the helical regions, which

presumably leads to a similar architecture of the tertiary fold (Figure 1). They contain four (p15 and p16) or five (p18 and p19) helix-turn-helix (H-T-H) motifs stacking together *via* hydrophobic interactions. A long, solvent-exposed loop, which is perpendicular to the molecular long axis, connects neighboring H-T-H motifs.

Despite structural homology, p16 and p15 (which are well-established tumor suppressors) show a high degree of conformational flexibility and a strong tendency to aggregate, while the larger proteins, p18 and p19 (which have rarely been found altered in tumor cells), display such properties to a far lesser degree. As a result of these differences, structural determination of p18 or p19 by either NMR or X-ray has not been uncommonly intractable (Luh *et al.*, 1997; Baumgartner *et al.*, 1998; Venkataramani *et al.*, 1998; Li *et al.*, 1999), whereas that of p16 or p15 has proven very difficult by either technique. No crystal structure of free p16 or p15 has been reported to date, despite extensive effort by several groups. The solution structure of p16 was also pursued by many laboratories and was first reported at a relatively low resolution (Byeon *et al.*, 1998), which has been refined to a higher resolution only recently (unpublished results). The solution structure of p15 could not be solved by NMR data alone, but required comparative modeling to complete the effort (unpublished results).

The problems associated with p16 and p15 have been described in our previous publications (Tevelev *et al.*, 1996; Byeon *et al.*, 1998). In summary, there are few or no detectable slowly

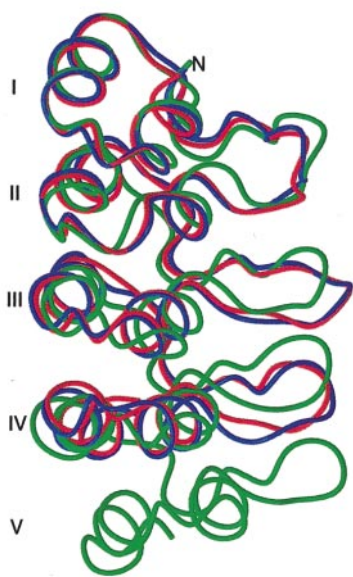


**Figure 1.** Overlay of ribbon diagrams of p15, p16, and p18 solution structures with the ankyrin repeats numbered. The Figure was generated with the Insight II software (Molecular Simulations Inc.).

exchanging amide protons in routine one-dimensional proton NMR spectra (conducted at 293 K), which is indicative of conformational flexibility. At concentrations above 0.4 mM the proteins aggregate severely as evidenced by line broadening. Thus all NMR experiments had to be performed at 0.2-0.4 mM, which required long acquisition times. As a further difficulty, the protein samples (most of them are <sup>15</sup>N or <sup>15</sup>N/<sup>13</sup>C-labeled) usually suffer irreversible denaturation during long-term data acquisition.

Our observations have been echoed by other reports (Boice & Fairman, 1996; Zhang & Peng, 1996). Recently, two in-depth studies have been reported. One of them deals with the backbone dynamics of p19 as investigated by <sup>15</sup>N NMR relaxation experiments (Renner *et al.*, 1998). It was reported that p19 has very limited conformational flexibility on the pico- to nanosecond time-scale. The other study (Tang *et al.*, 1999) uses circular dichroism (CD) and fluorescence studies to show that p16 exhibits both thermodynamic and kinetic instability.

Despite such in-depth studies, three key questions remain to be answered. (a) What are the specific physical parameters responsible for the problems associated with p16 and p15? (b) What are the quantitative differences in these physical parameters between the smaller members and the larger members of the family? (c) What are the structural bases of the differences in these physical parameters? The aim of this work is to gain further insight into these questions through a systematic and comparative study, which can enhance our understanding of the structure-function relationship of not only INK4 proteins, but also the large family of ankyrin-repeat proteins (Sedgwick & Smerdon, 1999). The conformational stability and flexibility of human p16 and human p18 were examined and compared as follows. (a) The thermodynamic stability of the protein was measured by guanidine hydrochloride (GdnHCl)-induced denaturation and the free energy of unfolding determined. (b) <sup>1</sup>H-<sup>15</sup>N nuclear Overhauser effect (NOE) experiments were carried out to probe the backbone flexibility on the pico- to nanosecond time-scale. (c) Hydrogen-deuterium exchange (<sup>1</sup>H/<sup>2</sup>H exchange) rates were measured by heteronuclear NMR spectroscopy to examine the conformational flexibility of p16 and p18 (as well as mouse p15) on a slower time-scale, i.e. minutes to hours.

## Results and Discussion

### Comparison of aggregation tendency and stability between p15, p16, and p18

Although we stated in the Introduction that p15, p16, and p18 differ in their aggregation tendency and stability during various NMR experiments, it is important to demonstrate such differences under identical and well-controlled conditions. At

0.8 mM, the line widths of the 1D proton NMR spectra of in <sup>2</sup>H<sub>2</sub>O are clearly broader for p16 than p18 (spectra not shown). We then used <sup>1</sup>H-<sup>15</sup>N heteronuclear single quantum coherence (HSQC) spectra to monitor the long-term stability of p15, p16, and p18 (in H<sub>2</sub>O) as shown in Figure 2. Approximately 50 spectra were taken for each, but only the first and a representative spectra are shown. It is clear that p15 lost most of the cross-peaks after seven days, p16 lost ca 50% of them after seven days, while p18 retains most of the peaks even after 21 days. Some of the remaining peaks for p16 arise from random coil conformations. The sample half-lives at room temperature are estimated to be three days for p15, seven days for p16, and 50 days for p18. The results demonstrate that the order of the "stability" of the three proteins is p15 < p16 < p18. The specific mechanism for the disappearance of NH cross-peaks is not clear, but it is most likely caused by a combination of aggregation, local denaturation, and unfolding. The samples were all clear (without precipitation) during the course of the experiments.

The results shown in Figure 2 also serve as a control for all of the experiments reported in this study, i.e. that they were performed well within the time constraint of stability.

### Conformational stability of p16 and p18 from denaturation experiments is small but similar

Protein denaturation by GdnHCl was monitored by CD spectroscopy in the far-UV region. The experiments for both p16 and p18 were carried out under the same conditions to eliminate the salt effect (Tang *et al.*, 1999). Figure 3 shows the CD denaturation curves of ellipticity at 222 nm *versus* GdnHCl concentration as well as the fitting results by using SigmaPlot software 4.0 (SPSS Inc.). The values of  $\Delta G_d^{\text{H}_2\text{O}}$  and slope  $m$  for p16 are 1.94(±0.10) kcal/mol and 3.23(±0.17) kcal mol<sup>-1</sup> M<sup>-1</sup>, respectively, while the corresponding values for p18 are 2.98(±0.18) kcal/mol and

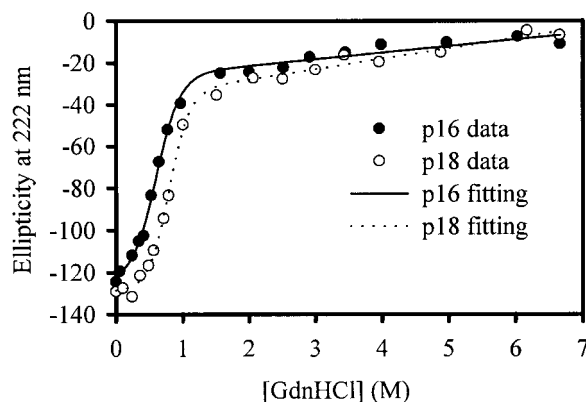


**Figure 3.** GdnHCl-induced denaturation curves of p16 and p18 at 293 K monitored by far-UV CD. Details of data collection are given in Materials and Methods. The data were fitted to equation (7) to obtain the conformational stability.

3.77(±0.24) kcal mol<sup>-1</sup> M<sup>-1</sup>. The results for full-length p16 obtained here are in excellent agreement with those for the truncated version (p16/ $\Delta$ 1-8) after baseline correction (Tevelev *et al.*, 1996). It is clear that the free energy of unfolding is relatively small for the two proteins, since the value for most proteins falls within 5-15 kcal/mol. Furthermore, p18 is about 1 kcal/mol more stable than p16, which could be attributed to the extra ankyrin repeat in p18. It appears questionable, however, that the small difference in thermodynamic stability is solely responsible for the markedly different behaviors of these two proteins.

### The p16 protein has very limited conformational flexibility on the time-scale of pico- to nanoseconds

In high magnetic field, the <sup>1</sup>H-<sup>15</sup>N steady-state NOE is dominated by the dipolar interaction and

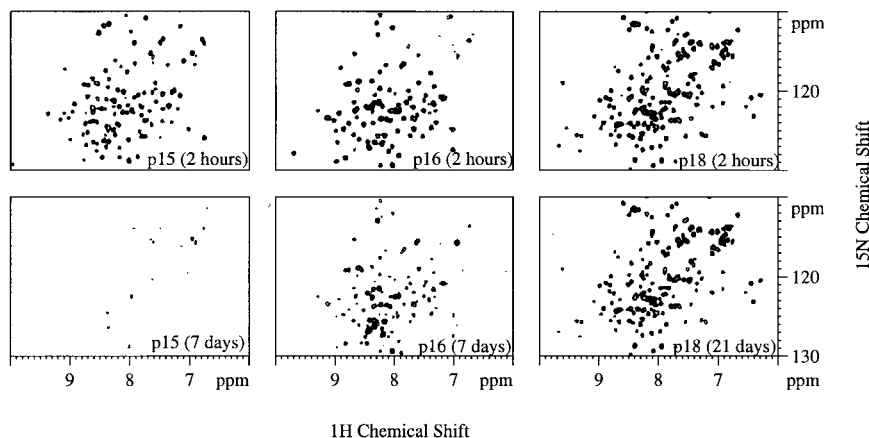


**Figure 2.** Use of <sup>1</sup>H-<sup>15</sup>N HSQC experiments to monitor the stability of sample lifetime of <sup>15</sup>N-labeled p15, p16 and p18 in <sup>2</sup>H<sub>2</sub>O on very long time-scales at room temperature (~298 K).

chemical shift anisotropy (Abragam, 1961). It is a sensitive probe of the backbone conformational flexibility on the pico- to nanosecond time-scale for a protein with a rotational correlation time on the nanosecond time-scale (Kay *et al.*, 1989). For the size of p16 and p18, the overall rotational correlation time ( $\tau_m$ ) is expected to be around 8 ns under the experimental conditions. A possible range for NOE can be estimated by using model-free formalism (Lipari & Szabo, 1982a,b), which gives an NOE value around 0.82 for a rigid backbone NH vector and a negative NOE around  $-3.50$  for an unrestricted one. A smaller number generally means greater flexibility of the measured backbone amide on the time-scale of pico- to nanoseconds.

Of the expected 144 backbone resonances of p16, 111 were quantitatively determined, as shown in Figure 4(a). In summary, the residues in the  $\alpha$ -helical conformation (residues 15-21, 25-33, 48-51, 57-65, 81-87, 91-99, 114-120, and 124-133) have an average NOE value of  $0.80(\pm 0.04)$ , while the residues in the turns or loops between D14 and A133 have an average of  $0.78(\pm 0.04)$  (excluding residue G111, 0.23). Starting at A134, the NOE values in the C-terminal region gradually approach zero and eventually become negative.

The magnitudes of NOE values depicted in Figure 3(a) suggest that the p16 protein retains an NOE feature characteristic of a rigid protein on the pico- to nanosecond time-scale, as explained below. (a) Most of the backbone amide protons in the stacked four ankyrin repeats have very limited conformational flexibility on the time-scale probed by heteronuclear NOE (pico- to nanoseconds). (b) Statistically, there is not much difference between residues in H-T-H motifs and in loop regions in terms of pico- to nanosecond flexibility.

(c) The only exception is the C terminus (residues 134-156) as well as a few residues at the N terminus, which are clearly in a highly flexible, unstructured conformation.

### Conformational flexibility on the pico- to nanosecond time-scale are comparable among INK4 proteins

The corresponding NOE data for p18 were determined in the same way and the results are illustrated in Figure 4(b). A total of 130 of the 163 possible backbone amide protons have been measured. The average values of the helical residues (residues 8-15, 18-26, 41-44, 50-58, 73-79, 83-91, 106-112, 116-123, 140-147, and 150-158) and the rest in the five ankyrin repeats are both  $0.79(\pm 0.05)$ , excluding three unusually low values (G38, 0.19; K66, 0.27; G131,  $-0.04$ ). The rigidity of p18 on the pico- to nanosecond time-scale is thus comparable to that of the four ankyrin repeats in p16, except that the highly flexible segments are shortened to less than ten residues in both the N and C termini of p18 relative to p16.

It has been shown that the p19 backbone exists as a well-defined structure of limited conformational flexibility on the pico- to nanosecond time-scale (Kalus *et al.*, 1997; Renner *et al.*, 1998). Our data, taken together with the reports cited above, are sufficient to rule out the possibility that fast internal motion or flexibility on this time-scale is responsible for the different behaviors between the smaller and the larger members of the INK4 proteins, particularly with respect to structural determination by NMR.

The reasons for the unusually low NOE values of a few residues (G111 in p16, G38, K66, and G131 in p18) are not clear. While they could be caused by peak-overlap with unassigned, flexible

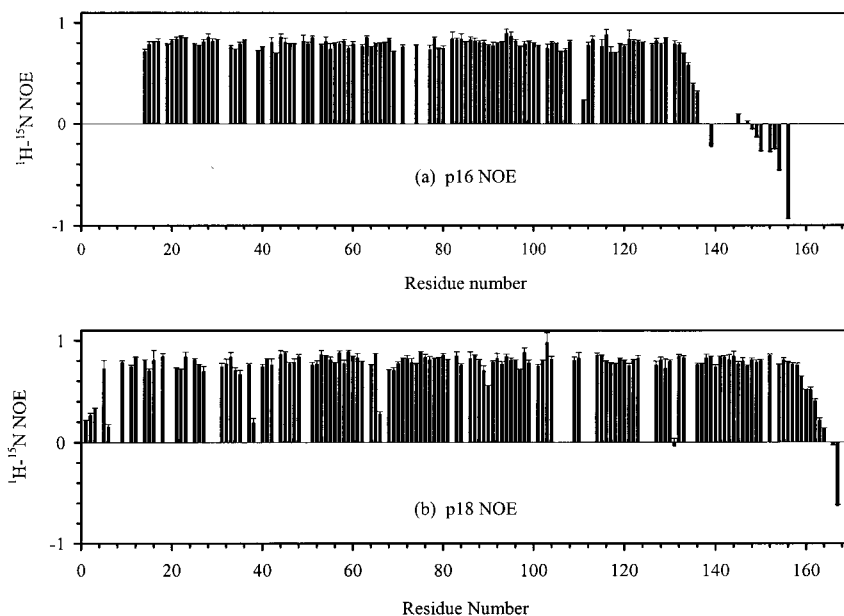


**Figure 4.** Plots of  $^1\text{H}-^{15}\text{N}$  steady-state heteronuclear NOE as a function of residue number for (a) p16 and (b) p18. The experiments were performed on a Bruker DMX-600 NMR spectrometer at 293 K.

terminal residues, a functional implication could not be ruled out, since the first three residues are neighbors of binding residues (Russo *et al.*, 1998). This warrants a more detailed study, such as performing  $T_1$  and  $T_2$  measurements (Renner *et al.*, 1998). The outcome of such analyses, however, should not affect the conclusion of this work.

### H/<sup>2</sup>H exchange rates are significantly different for INK4 proteins

The most significant results in this work come from hydrogen-deuterium exchange experiments monitored by NMR spectroscopy. The exchange rates of amide protons were measured for three INK4 proteins (p15, p16, and p18) at physiological pH (pH 7.5). To slow down the exchange rate, the experimental temperature was lowered to 283 K from the normally used 293 K. The H/<sup>2</sup>H exchange rates of the three proteins can be qualitatively compared by inspection of the <sup>1</sup>H-<sup>15</sup>N HSQC spectra. As shown in Figure 5 the H/<sup>2</sup>H exchange rates clearly follow the order of p15 ≥ p16 > p18. For p15, all the amide peaks were exchanged within two hours. p16 amide exchange rates are somewhat slower: it takes about ten hours to exchange all the amide protons. p18 undergoes the slowest amide exchange: it takes > seven days to exchange all the amide protons to deuterium (later spectra not shown in Figure 5).

For well-resolved <sup>1</sup>H-<sup>15</sup>N cross-peaks, H/<sup>2</sup>H exchange rates were quantitatively determined. The peak volumes were measured using Felix 97, and the H/<sup>2</sup>H exchange rates were extracted by fit-

ting the time-course data to a single-exponential function using SigmaPlot software 4.0:

$$y = A \exp(-k_{\text{ex}}t) + B \quad (1)$$

where  $k_{\text{ex}}$  is the rate constant;  $y$  represents the peak volume at time  $t$ , and  $t$  is the time elapsed in <sup>2</sup>H<sub>2</sub>O from the beginning to the middle of each data acquisition. Representative plots of decay curves and data fitting are shown in Figure 6. The fitting results for specific residues are listed in a long table in the Supplementary Material. A short summary of these data is shown in Table 1. Overall, the rate constants for exchange ( $k_{\text{ex}}$ ) for the residues analyzed fall into the range of  $11 \times 10^{-3}$  to  $52 \times 10^{-3} \text{ min}^{-1}$  for p15, with an average value of  $20 \times 10^{-3} \text{ min}^{-1}$ , and  $2.6 \times 10^{-3}$  to  $54 \times 10^{-3} \text{ min}^{-1}$  for p16, with an average of  $12 \times 10^{-3} \text{ min}^{-1}$ . The  $k_{\text{ex}}$  values in p18 are ca  $5 \times 10^{-3} \text{ min}^{-1}$  for most residues, except that one set of residues could not be fitted well with equation (1) as  $B$  (the baseline correction factor) is comparable to  $A$ , the volume at time zero. These residues, the significance of which will be elaborated upon below, decay very slowly within the experimental time (4600 minutes). Their  $k_{\text{ex}}$  was thus estimated by using the single-exponential function of  $y = A \exp(-k_{\text{ex}}t)$  (e.g. E120 of p18 in Figure 6(c)).

To quantitatively compare the overall H/<sup>2</sup>H exchange rates of the three proteins, we also integrated the whole peak area of each sample and fit the time-course of total peak volume to equation (1). The fitting gives  $20(\pm 2) \times 10^{-3}$ ,  $9.0(\pm 0.5) \times 10^{-3}$ , and  $2.3(\pm 0.1) \times 10^{-3} \text{ min}^{-1}$  for p15, p16 and p18, respectively (Figure 7).

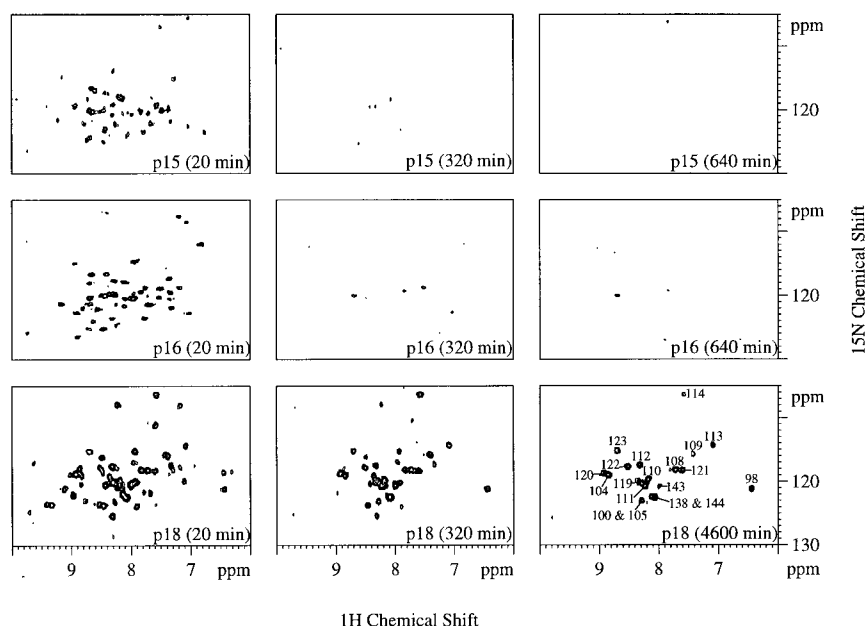


**Figure 5.** Contour plots of the <sup>1</sup>H-<sup>15</sup>N HSQC spectra of p15, p16, and p18 samples, pH 7.5 at 283 K after exchange with <sup>2</sup>H<sub>2</sub>O for the time indicated in each spectrum. The proteins were freshly dissolved in <sup>2</sup>H<sub>2</sub>O after lyophilization from a H<sub>2</sub>O solution. Details of data collection are given in Materials and Methods. The HSQC spectrum of p18 at the latest time-point (4600 minutes) was labeled with assignments based on previous results (Li *et al.*, 1999).

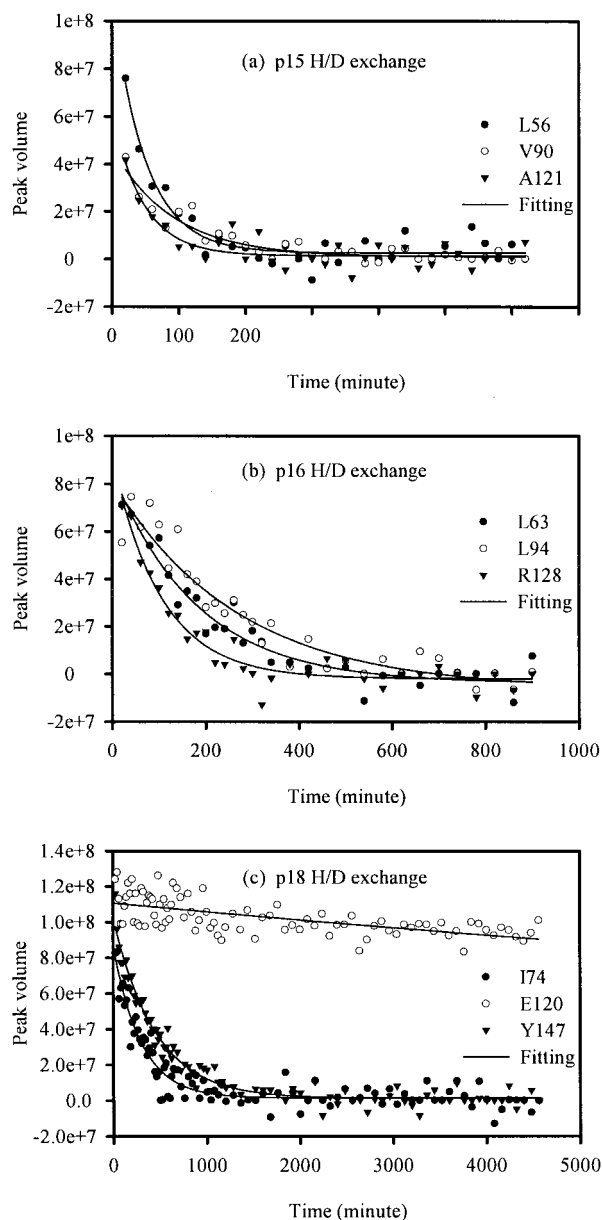


**Figure 6.** Representative plots showing the decay curves ( $^{15}\text{N}$ - $^1\text{H}$  HSQC cross-peak volumes *versus* time) and the fitting for selected residues in (a) p15, (b) p16, and (c) p18. The peak volumes were measured by using Felix 97 (Molecular Simulations Inc.). The data were fitted to equation (1) using SigmaPlot software 4.0 (SPSS Inc.), except that of E120 in p18 was fitted to:

$$y = A \exp(-k_{\text{ex}}t)$$

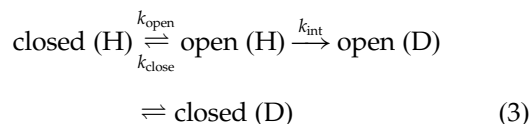
However, as we can see from Figure 7, the fitting of p18 failed to delineate the slow volume decay at long experimental time (>700 minutes). Thus we repeated the data fitting according to the following equation:

$$y = A_1 \exp(-k_{\text{ex}1}t) + A_2 \exp(-k_{\text{ex}2}t) \quad (2)$$

which gives two rate constants:  $3.7(\pm 0.2) \times 10^{-3}$  and  $0.11(\pm 0.01) \times 10^{-3} \text{ min}^{-1}$ . The latter accounts for the behavior of slowly exchanging amide protons in p18.

### Differences in H/ $^2\text{H}$ exchange rate reflect differences in kinetic stability

It has been established that a general two-process model could be used to describe the H/ $^2\text{H}$  exchange behavior of a native folded protein with solvent (Woodward & Hilton, 1980; Clarke & Itzhaki, 1998). In this model, there exists an equilibrium step between folded (closed form) and unfolded (transient open form, either locally or globally) conformations, while solvent exchange only takes place in the open form:



Here  $k_{\text{open}}$ ,  $k_{\text{close}}$  and  $k_{\text{int}}$  refer to the opening rate, closing rate, and the intrinsic exchange rate from the open species, respectively. The apparent exchange rate ( $k_{\text{ex}}$ ) is expressed by the following equation:

$$k_{\text{ex}} = \frac{k_{\text{open}}k_{\text{int}}}{k_{\text{close}} + k_{\text{int}}} \quad (4)$$

Two limits are typically approximated, in which the exchange rate is expressed as:  $k_{\text{ex}} = k_{\text{open}}$  (EX1 limit when  $k_{\text{int}} \gg k_{\text{close}}$ ) and  $k_{\text{ex}} = k_{\text{int}}k_{\text{open}}/k_{\text{close}} = k_{\text{int}}K_{\text{open}}$  (EX2 limit when  $k_{\text{close}} \gg k_{\text{int}}$ ). In our work two conditions favor the EX1 limit: the low  $\Delta G_{\text{d}}^{\text{H}_2\text{O}}$  and high pH used (Swint-Kruse & Robertson, 1996; Clarke & Itzhaki, 1998). The analyses in the following paragraphs further show that our system is far from the EX2 limit.

The intrinsic exchange rates ( $k_{\text{int}}$ ) can be calculated from the free peptide exchange rates with correction for the effects of primary sequence, pH and temperature (Bai *et al.*, 1993). Under our experimental conditions (neutral pH), the H/ $^2\text{H}$  exchange is dominated by a base-catalyzed mechanism and the majority of  $k_{\text{int}}$  falls in the range of 100-600  $\text{min}^{-1}$  (Bai *et al.*, 1993). The protection factor (PF) expressed as  $\text{PF} = k_{\text{int}}/k_{\text{ex}}$  was then calculated for each quantitatively analyzed residue. Usually a larger protection factor indicates lower flexibility for a particular residue. It was found that even in p15 the PF could be as high as the order of  $10^4$  (Table 1). Assuming an EX2 limit, the free energy of H/ $^2\text{H}$  exchange,  $\Delta G_{\text{ex}}$  can be calculated as  $\Delta G_{\text{ex}} = -RT \ln(K_{\text{open}}) = RT \ln(\text{PF})$ . It was reported that most of the H/ $^2\text{H}$  exchange studies for which the EX2 limit applies show a good correlation between  $\Delta G_{\text{ex}}$  and  $\Delta G_{\text{d}}^{\text{H}_2\text{O}}$  (Clarke & Itzhaki, 1998). By using the largest PF listed in Table 1, the

**Table 1.** Summary of H/<sup>2</sup>H exchange experiments

	p15	p16	P18
Number of residues observed beyond the experimental dead time (20 minutes)	44 (34 in helical conformation)	58 (45 in helical conformation)	68 (49 in helical conformation; 10 in loop 3)
Number of quantitatively analyzed residues	29	38	36 <sup>a</sup>
Average $k_{\text{ex}}$ (min <sup>-1</sup> )	$20 \times 10^{-3}$	$12 \times 10^{-3}$	$4.8 \times 10^{-3}$
Smallest $k_{\text{ex}}$ (min <sup>-1</sup> )	$11(\pm 2) \times 10^{-3}$	$2.6(\pm 0.8) \times 10^{-3}$	$2.4(\pm 1.0) \times 10^{-5}$
Average PF	$1.9 \times 10^4$	$4.7 \times 10^4$	$1.0 \times 10^6$
Largest PF	$7.8 \times 10^4$	$2.3 \times 10^5$	$7.1 \times 10^6$

<sup>a</sup>The  $k_{\text{ex}}$  values of seven residues were estimated by fitting the decay to the equation of  $y = A \exp(-k_{\text{ex}}t)$ .

$\Delta G_{\text{ex}}$  values of p15, p16, and p18 were calculated to be 6.3, 7.0, and 8.9 kcal/mol, respectively. These numbers are inconsistent with the low free energy determined by chemical denaturant unfolding.

In some cases, the inconsistency can be attributed to the *cis-trans* isomerization of a proline residue (Bai *et al.*, 1994; Mullins *et al.*, 1997). However there is no *cis*-proline observed in NMR studies of both p16 and p18. One may also argue that the free energy discrepancy arises from the fact that H/<sup>2</sup>H exchange rates were determined at a lower temperature (283K). However, we would not anticipate a very sharp dependence of  $\Delta G$  on temperature in the vicinity of physiological conditions, since the heat capacity changes were estimated to be approximately  $1.9 \text{ kcal mol}^{-1} \text{ K}^{-1}$  from slope  $m$  values using an empirical relationship (Myers *et al.*, 1995).

The difference in H/<sup>2</sup>H exchange rate thus reflects mainly the difference in the unfolding kinetic barrier or kinetic stability (EX1 limit) rather than that of the thermodynamic stability (EX2 limit). We can conclude from the H/<sup>2</sup>H exchange data that the following order exists:  $k_{\text{open}}$  (p15)  $\geq k_{\text{open}}$  (p16)  $> k_{\text{open}}$  (p18). For an individual residue,  $k_{\text{open}}$  is the sum of  $k_{\text{open}}$  (local) and  $k_{\text{open}}$  (global). Assuming that the slowest amide in each protein is controlled by the transient global unfolding, in other words, the smallest  $k_{\text{ex}}$  is equal to the global transient  $k_{\text{open}}$ (global), then the ratio of  $k_{\text{open}}$ (global) is roughly 400:100:1 for p15, p16 and p18. In conclusion, while the INK4 proteins may have similar low thermodynamic stability as shown by GdnHCl denaturation of p16 and p18, they probably display markedly different kinetic stability, i.e. p18  $>$  p16  $\geq$  p15.

### Structural basis for the difference between p16 and p18

It was postulated that a minimal number of ankyrin repeats is required to provide stabilizing interactions between the helices and  $\beta$ -strands of adjacent modules in the ankyrin repeat structures (McDonald & Peters, 1998). As elaborated below, the results presented here support that an additional ankyrin unit enhances the protein stability (thermodynamic as well as kinetic). The stabi-

lizing effect is particularly apparent in the fourth ankyrin repeat of p18.

There are as many as 19 peaks that show residual signals in the HSQC spectrum of the p18 sample after 4600 minutes of H/<sup>2</sup>H exchange at 283 K (Figure 5). Their half-lives are estimated to be longer than 6900 minutes (or  $k_{\text{ex}} \leq 1 \times 10^{-4} \text{ min}^{-1}$ ). Based on previous resonance assignments (Li *et al.*, 1999) they have been assigned as follows: I98, D100, N104, L105, H108, L109, A110, A111, K112, E113, G114, V119, E120, F121, L122, V123, D138, L143, and A144. Clearly these residues are clustered in the region of the fourth ankyrin repeat (Figure 1).

The role of the C-terminal segment in INK4 structural integrity is further highlighted here. It is likely that additional residues in an unstructured form may still contribute somewhat to the conformational stability of the protein. Compared with p15, p16 has an additional 20 residues in the C terminus which, though relatively unstructured, could be related to the fact that p16 shows somewhat slower H/<sup>2</sup>H exchange rates and a decreased aggregation tendency relative to p15. This is supported by our previous report that deletion of these C-terminal residues enhanced the tendency of p16 to aggregate (Tevelev *et al.*, 1996). However, the argument in this section does not rule out the possibility of different contributions from the first four ankyrin repeats among INK4 proteins.

Another interesting point is that the majority of the amide NH protons observed beyond the experimental dead time (20 minutes) are helical residues in all the three proteins. However, in p18 as many as ten residues were found in loop 3.

### Possible relationship between conformational flexibility and aggregation

Structural determination of proteins by NMR has been plagued by aggregation, a natural property of many proteins (Wagner, 1993). Although there are no accurate statistical data, it is estimated that the structures of more than 50% of proteins with appropriate size could not be determined by NMR because of aggregation. It is commonly believed that aggregation is caused by surface-surface interaction, either electrostatic or hydrophobic in nature, between different protein molecules.

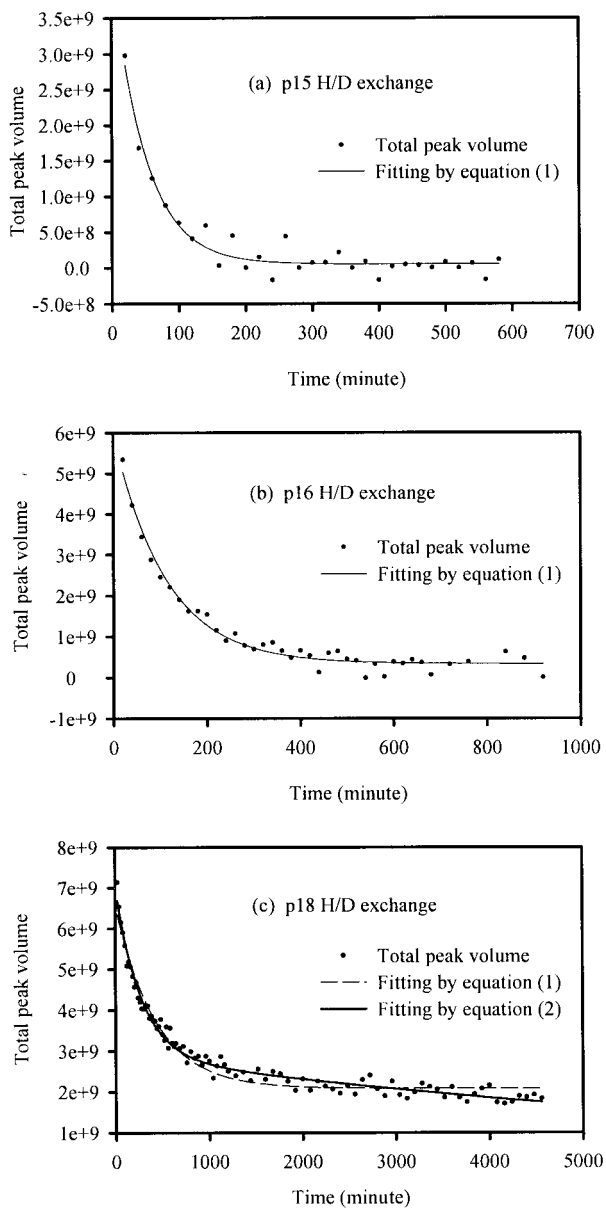
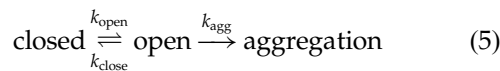


**Figure 7.** Overall H/<sup>2</sup>H exchange rate constants extracted by fitting the time-course data of total peak volumes to equation (1) for p15 and p16 and to equation (1) as well as equation (2) for p18.

While this could very well be a general mechanism of protein aggregation, it is not evident in our system. As described in our first paper (Tevelev *et al.*, 1996), we have constructed mutants aimed at reducing hydrophobic interactions on the surface of p16. The result was always the opposite, i.e. the mutants aggregate and denature more severely, possibly because the mutation made the protein more flexible.

Since the conformational flexibility (as measured by H/<sup>2</sup>H exchange) and the aggregation tendency both follow the same order p15 ≥ p16 > p18, our results suggest that conformational flexibility could

enhance the aggregation tendency for INK4 proteins. This could be explained by the following model:



In this model, irreversible aggregation occurs following transient global opening of native protein. The apparent aggregation rate, in analogy to the H/<sup>2</sup>H exchange mechanism, can be expressed as:

$$\begin{aligned} k_{\text{agg}}(\text{apparent}) &= \frac{k_{\text{open}}k_{\text{agg}}}{k_{\text{close}} + k_{\text{agg}}} \\ &= \frac{k_{\text{agg}}}{\exp(\Delta G_{\text{D}}^{\text{H}_2\text{O}}/RT) + \frac{k_{\text{agg}}}{k_{\text{open}}}} \quad (6) \end{aligned}$$

If it is assumed that the  $k_{\text{agg}}$  values of all INK4 proteins are similar, two factors can contribute to higher  $k_{\text{agg}}$  (apparent) for p16 and p15 relative to p18. The first factor is thermodynamic; the first term in the denominator is about five times smaller for p16 than for p18 based on the denaturation results. The second factor is kinetic; the second term in the denominator ( $k_{\text{agg}}/k_{\text{open}}$ ) is also smaller for p16 due to larger  $k_{\text{open}}$  as described above. When  $k_{\text{agg}}$  is comparable to or greater than  $k_{\text{close}}$ , which may be possible since INK4 proteins are aggregation-prone, the kinetic factor would contribute more to the different aggregation tendency of INK4 proteins because the differences in the  $k_{\text{open}}$  values are large (~two orders of magnitude).

### Comparison of the three experimental approaches

Heteronuclear relaxation measurements and H/<sup>2</sup>H exchange are two popular approaches to elucidate conformational properties of proteins. While the former yields information on protein internal motions on the pico- to nanosecond time-scales (Kay *et al.*, 1989; Palmer, 1997), the latter is often used to establish dynamic processes on the time-scale of minutes to hundreds of hours (Englander & Kallenbach, 1984). Our results suggest that the H/<sup>2</sup>H exchange rate is more relevant to the “practical behavior” of the INK4 proteins. The third property, free energy of unfolding, is a thermodynamic property that may not be directly related to the H/<sup>2</sup>H exchange rates under the EX1 limit.

Although the studies were performed mostly on p16 and p18, the conclusion may be extended to the entire INK4 family and other ankyrin-repeat proteins. Overall, INK4 proteins may all be thermodynamically unstable with comparable free energies of unfolding. They also likely behave similarly in terms of pico- to nanosecond dynamics. Major differences among these proteins lie in the H/<sup>2</sup>H exchange rates, which are substantially faster for smaller members of the family, and which

correlate with unfolding kinetic barrier or kinetic stability. Thus the differences in kinetic stability probably are mainly responsible for the markedly different behaviors between smaller proteins and larger proteins of the INK4 family. From the structural point of view, this difference is likely caused by the additional ankyrin in p18 and p19.

## Materials and Methods

### Protein sample preparation

The proteins (p15, p16, and p18) were all expressed in a soluble form as a glutathione *S*-transferase (GST) fusion protein in *Escherichia coli* BL21 (DE3) (Novagene). The GST portion was cleaved off with thrombin and the proteins were purified as described (Byeon *et al.*, 1998; Li *et al.*, 1999). The uniformly <sup>15</sup>N-labeled proteins were prepared by growing host cells in M9 minimal medium with (<sup>15</sup>NH<sub>4</sub>)<sub>2</sub>SO<sub>4</sub> as the only nitrogen source (Muchmore *et al.*, 1989).

### Conformational stability of p16 and p18 measured by CD

Lyophilized proteins were dissolved in borate buffer (20 mM sodium borate, 40 μM dithioerythritol, pH 7.5) followed by dialyzing overnight twice against two liters of the same buffer to remove other salts. A stock solution of GdnHCl near 8.5 M was prepared in the same borate buffer. Both protein sample and GdnHCl solution, along with the buffer, were used to prepare 18 different solutions with the same protein concentration (~10.0 μM) but with different GdnHCl concentrations ranging from 0 to around 7 M. The exact concentration of GdnHCl was determined by refractive index (Nozaki, 1972). Samples were then incubated on ice overnight prior to measurement. Far-UV CD spectra (200–250 nm) were recorded on a JASCO J-500C spectropolarimeter using a quartz microcell of 1 cm length. The measurements were carried out at 293 K in a thermostatically controlled cell holder with conditions of 20 nm/minute, step resolution 0.2 nm, band width 2.0 nm, and ten scans for each point. The ellipticity at 222 nm was taken as the measure of the degree of structure present in the protein at each GdnHCl concentration. Assuming a two-state model, the conformational stability in H<sub>2</sub>O, Δ*G*<sub>d</sub><sup>H<sub>2</sub>O</sup>, was obtained by fitting the data to the following equation, which has a correction for baseline only above the transition (Pace, 1986; Clarke & Fersht, 1993):

ε =

$$\frac{\varepsilon_F + (\alpha + \beta[\text{GdnHCl}]) \times \exp\{(m[\text{GdnHCl}] - \Delta G_d^{\text{H}_2\text{O}})/RT\}}{1 + \exp\{(m[\text{GdnHCl}] - \Delta G_d^{\text{H}_2\text{O}})/RT\}} \quad (7)$$

Here ε represents the ellipticity value at a given denaturant concentration, ε<sub>F</sub> and ε<sub>U</sub> (ε<sub>U</sub> = α + β[GdnHCl]) are the respective values of folded and unfolded forms, and the slope *m* is a constant related to the susceptibility of the protein toward denaturation by the denaturant (Myers *et al.*, 1995). The constants of α and β can be extracted from the linear fitting of the final eight points.

### Heteronuclear <sup>1</sup>H-<sup>15</sup>N NOE experiment

All NMR experiments were performed on a Bruker DMX600 spectrometer, which was equipped with a 5 mm triple-resonance probe with three-axes gradients. Unless stated otherwise, the NMR samples contained 0.2 mM <sup>15</sup>N-uniformly labeled protein (p16 and p18), 4 mM *N*-[2-hydroxyethyl]piperazine-*N'*-[2-ethanesulfonic] acid (Hepes), 1 mM dithioerythritol (DTE), and 5 μM ethylenediaminetetraacetic acid (EDTA) in 95% H<sub>2</sub>O/5% <sup>2</sup>H<sub>2</sub>O at pH 7.5. The <sup>1</sup>H-<sup>15</sup>N steady-state heteronuclear NOE experiments were carried out on both p16 and p18 at 293 K using the pulse sequence with a water flip-back version (Grzesiek & Bax, 1993). To minimize differences in sample conditions, two spectra were recorded in an interleaved manner: one with proton saturation (NOE effect) and one without proton saturation (without NOE effect). Each spectrum consists of a 128\* (*t*<sub>1</sub>) by 1024\* (*t*<sub>2</sub>) data matrix with acquisition times of 60.1 ms (*t*<sub>1</sub>) and 122.1 ms (*t*<sub>2</sub>). A recycle delay of three seconds was used to ensure the recovery of magnetization during the delay. The data were processed with Felix 97 (Molecular Simulation Inc., 1997) installed on a Silicon Graphics O2 computer. Briefly, each data set was zero-filled to 256 by 2048 data points, multiplied by a 90° shifted sinebell function in both dimension followed by Fourier transformation. The NOE values were calculated as NOE = (*I*<sub>w</sub>/*I*<sub>w0</sub>), where *I*<sub>w</sub> and *I*<sub>w0</sub> are the peak intensities recorded with and without proton presaturation respectively. The average values and errors were determined from two separate measurements.

### H/<sup>2</sup>H exchange NMR experiments

The lyophilized uniformly <sup>15</sup>N-labeled proteins (p15, p16 and p18) were dissolved into 99.99% <sup>2</sup>H<sub>2</sub>O (Cambridge Isotope) on ice and quickly placed in the probe, which was pre-equilibrated at 283 K, to initiate H/<sup>2</sup>H exchange. The first <sup>15</sup>N-<sup>1</sup>H HSQC experiment was started ten minutes after incubating the protein in the probe. The water flip-back HSQC pulse sequence was used (Grzesiek & Bax, 1993). Relaxation time between scans was 1.2 seconds. Each data set consisted of 32\* (*t*<sub>1</sub>) by 1024\* (*t*<sub>2</sub>) data points with acquisition times of 15.0 ms (*t*<sub>1</sub>) and 122.1 ms (*t*<sub>2</sub>). The spectral width in the proton dimension (*f*<sub>2</sub>) was 8389.3 Hz, and the spectral width in the nitrogen dimension (*f*<sub>1</sub>) was 2128.6 Hz. The total experimental time for each HSQC with eight scans/*t*<sub>1</sub> increment was 20 minutes. The subsequent experiments were obtained every 20 minutes. The data were processed and the peak volumes were measured using Felix 97 (Molecular Simulations Inc.).

### Probing the aggregation rates

The <sup>15</sup>N-labeled samples (p15, p16, and p18) were dissolved into 90% H<sub>2</sub>O/10% <sup>2</sup>H<sub>2</sub>O with a concentration of 0.2 mM. <sup>1</sup>H-<sup>15</sup>N HSQC was carried out to monitor the lifetime of each native protein on a very long time-scale (>one month). In a separate experiment, non-labeled p16 and p18 were dissolved into 99.99% <sup>2</sup>H<sub>2</sub>O (Cambridge Isotope) with a concentration of 0.8 mM. They were monitored by one-dimensional proton NMR and NOESY experiment. While all the experiments were performed at 293 K, samples were stored at room temperature (~298 K).

## Acknowledgments

The authors thank Alex Showalter for a critical reading of the manuscript and Dr Nico Tjandra for providing the pulse sequence of heteronuclear NOE experiments. This work was supported by NIH grant CA 69472 to M.-D.T. and American Cancer Society grant IRG 16-33 to I.-J.L.B. The study made use of a Bruker DMX-600 NMR spectrometer funded by NIH grant RR 08299 and NSF Grant BIR-9221639.

## References

- Abragam, A. (1961). *Principles of Nuclear Magnetism*, Clarendon Press, Oxford, UK.
- Bai, Y., Milne, J. S., Mayne, L. & Englander, S. W. (1993). Primary structure effects on peptide group hydrogen exchange. *Proteins: Struct. Funct. Genet.* **17**, 75-86.
- Bai, Y., Milne, J. S., Mayne, L. & Englander, S. W. (1994). Protein stability parameters measured by hydrogen exchange. *Proteins: Struct. Funct. Genet.* **20**, 4-14.
- Baumgartner, R., Fernandez-Catalan, C., Winoto, A., Huber, R., Engh, R. A. & Holak, T. A. (1998). Structure of human cyclin-dependent kinase inhibitor p19<sup>INK4d</sup>: comparison to known ankyrin-repeat-containing structures and implications for the dysfunction of tumor suppressor p16<sup>INK4a</sup>. *Structure*, **6**, 1279-1290.
- Boice, J. A. & Fairman, R. (1996). Structural characterization of the tumor-suppressor p16, an ankyrin-like repeat protein. *Protein Sci.* **5**, 1776-1784.
- Byeon, I.-J. L., Li, J., Ericson, K., Selby, T. L., Tevelev, A., Kim, H.-J., O'Maille, P. & Tsai, M.-D. (1998). Tumor suppressor p16<sup>INK4A</sup>: determination of solution structure and analyses of its interaction with cyclin-dependent kinase 4. *Mol. Cell.* **1**, 421-431.
- Clarke, J. & Fersht, A. R. (1993). Engineered disulfide bonds as probes of the folding pathway of barnase: increasing the stability of proteins against the rate of denaturation. *Biochemistry*, **32**, 4322-4329.
- Clarke, J. & Itzhaki, L. S. (1998). Hydrogen exchange and protein folding. *Curr. Opin. Struct. Biol.* **8**, 112-118.
- Englander, S. W. & Kallenbach, N. R. (1984). Hydrogen exchange and structural dynamics of protein and nucleic acids. *Quart. Rev. Biophys.* **16**, 521-655.
- Grzesiek, G. & Bax, A. (1993). The importance of not saturating H<sub>2</sub>O in protein NMR. Application to sensitivity enhancement and NOE measurements. *J. Am. Chem. Soc.* **115**, 12593-12594.
- Kalus, W., Baumgartner, R., Renner, C., Noegel, A., Chan, F. K. M., Winoto, A. & Holak, T. A. (1997). NMR structural characterization of the WK inhibitor p19<sup>INK4d</sup>. *FEBS Letters*, **401**, 127-132.
- Kay, L. E., Torchia, D. A. & Bax, A. (1989). Backbone dynamics of proteins as studied by <sup>15</sup>N inverse detected heteronuclear NMR spectroscopy: application to staphylococcal nuclease. *Biochemistry*, **28**, 8972-8979.
- Li, J., Byeon, I. J.-L., Ericson, K., Pol, M. J., O'Maille, R., Selby, T. & Tsai, M.-D. (1999). Tumor suppressor INK4: determination of the solution structure of p18<sup>INK4C</sup> and demonstration of the functional significance of loops in p18<sup>INK4C</sup> and p16<sup>INK4C</sup>. *Biochemistry*, **38**, 2930-2940.
- Lipari, G. & Szabo, A. (1982a). Model-free approach to the interpretation of nuclear magnetic resonance relaxation in macromolecules. 1. Theory and range of validity. *J. Am. Chem. Soc.* **104**, 4546-4559.
- Lipari, G. & Szabo, A. (1982b). Model-free approach to the interpretation of nuclear magnetic resonance relaxation in macromolecules. 2. Analysis of experimental results. *J. Am. Chem. Soc.* **104**, 4559-4570.
- Luh, F. Y., Archer, S. J., Domaille, P. J., Smith, B. O., Owen, D., Brotherton, D. H., Raine, A. R. C., Xu, X., Brizuela, L., Brenner, S. L. & Laue, E. D. (1997). Structure of the cyclin-dependent kinase inhibitor p19<sup>INK4d</sup>. *Nature*, **389**, 999-1003.
- McDonald, N. Q. & Peters, G. (1998). Ankyrin for clues about the function of p16<sup>INK4a</sup>. *Nature Struct. Biol.* **5**, 85-88.
- Muchmore, D. C., McIntosh, L. P., Russel, C. B., Anderson, D. E. & Dahlquist, F. W. (1989). Expression and nitrogen-15 labeling of proteins for proton and nitrogen-15 nuclear magnetic resonance. *Methods Enzymol.* **177**, 44-73.
- Mullins, L. S., Pace, C. N. & Raushel, F. M. (1997). Conformational stability of ribonuclease T1 determined by hydrogen-deuterium exchange. *Protein Sci.* **6**, 1387-1395.
- Myers, J. K., Pace, C. N. & Scholtz, J. M. (1995). Denaturant *m* values and heat capacity changes: relation to changes in accessible surface areas of protein unfolding. *Protein Sci.* **4**, 2138-2148.
- Nozaki, Y. (1972). The preparation of guanidine hydrochloride. *Methods Enzymol.* **26**, 43-50.
- Pace, C. N. (1986). Determination and analysis of urea and guanidine hydrochloride denaturation curves. *Methods Enzymol.* **131**, 266-279.
- Palmer, A. G. (1997). Probing molecular motion by NMR. *Curr. Opin. Struct. Biol.* **7**, 732-737.
- Renner, C., Baumgartner, R., Noegel, A. A. & Holak, T. A. (1998). Backbone dynamics of the CDK inhibitor p19<sup>INK4d</sup> studied by <sup>15</sup>N NMR relaxation experiments at two field strengths. *J. Mol. Biol.* **283**, 221-229.
- Russo, A. A., Tong, L., Lee, J. O., Jeffrey, P. D. & Pavletich, N. P. (1998). Structural basis for inhibition of the cyclin-dependent kinase Cdk6 by the tumour suppressor p16<sup>INK4a</sup>. *Nature*, **395**, 237-243.
- Sedgwick, S. G. & Smerdon, S. J. (1999). The ankyrin repeat: a diversity of interactions on a common structural framework. *Trends Biochem. Sci.* **24**, 311-316.
- Serrano, M., Hannon, G. J. & Beach, D. (1993). A new regulatory motif in cell-cycle control causing specific inhibition of cyclin D/CDK4. *Nature*, **366**, 704-707.
- Sherr, C. J. (1996). Cancer cell cycles. *Science*, **274**, 1672-1677.
- Swint-Kruse, L. & Robertson, A. D. (1996). Temperature and pH dependences of hydrogen exchange and global stability for ovomucoid third domain. *Biochemistry*, **35**, 171-180.
- Tang, K. S., Guralnick, B. L., Wang, W. K., Fersht, A. R. & Itzhaki, L. S. (1999). Stability and folding of the tumor suppressor protein p16. *J. Mol. Biol.* **285**, 1869-1886.
- Tevelev, A., Byeon, I.-J. L., Selby, T., Ericson, K., Kim, H.-J., Kraynov, V. & Tsai, M.-D. (1996). Tumor-suppressor p16<sup>INK4A</sup>: structural characterization of

- wild-type and mutant proteins by NMR and circular dichroism. *Biochemistry*, **35**, 9475-9487.
- Venkataramani, R., Swaminathan, K. & Mannorstein, R. (1998). Crystal structure of the CDK4/6 inhibitory protein p18<sup>INK4c</sup> provides insights into ankyrin-like repeat structure/function and tumor-derived p16<sup>INK4</sup> mutations. *Nature Struct. Biol.* **5**, 74-81.
- Wagner, G. (1993). Prospects for NMR of large proteins. *J. Biomol. NMR*, **3**, 375-385.
- Woodward, C. K. & Hilton, B. D. (1980). Hydrogen isotope exchange kinetics; of single protons in BPTI. *Biophys. J.* **32**, 561-575.
- Zhang, B. & Peng, Z. Y. (1996). Defective folding of mutant p16<sup>INK4</sup> proteins encoded by tumor-derived alleles. *J. Biol. Chem.* **271**, 28734-28737.

*Edited by P. E. Wright*

(Received 22 June 1999; received in revised form 23 September 1999; accepted 23 September 1999)



<http://www.academicpress.com/jmb>

Supplementary material comprising one Table is available from JMB Online.